Contents lists available at ScienceDirect

Biochemical and Biophysical Research Communications

journal homepage: www.elsevier.com/locate/ybbrc

Histone deacetylase 10 knockout activates chaperone-mediated autophagy and accelerates the decomposition of its substrate

Hitomi Obayashi [a], Yoshito Nagano [a, b, *], Tetsuya Takahashi [a], Takahiro Seki [c],
Shigeru Tanaka [d], Norio Sakai [d], Masayasu Matsumoto [e], Hirofumi Maruyama [a]

[a] Department of Clinical Neuroscience and Therapeutics, Graduate School of Biomedical and Health Sciences, Hiroshima University, Hiroshima, 734-8551, Japan
[b] Mitsubishi Tanabe Pharma, Osaka, 541-8505, Japan
[c] Department of Chemico-Pharmacological Sciences, Graduate School of Pharmaceutical Sciences, Kumamoto University, Kumamoto, 862-0973, Japan
[d] Department of Molecular and Pharmacological Neuroscience, Graduate School of Biomedical & Health Sciences, Hiroshima University, Hiroshima, 734-8551, Japan
[e] Sakai City Medical Center, Osaka, 593-8304, Japan

ARTICLE INFO

ABSTRACT

Histone deacetylase (HDAC) 10 is a member of class IIb HDACs, but its deacetylation targets and functions are poorly characterized. Recent investigation has proposed that HDAC10 deacetylates heat shock cognate protein 70 kDa (HSC70) after interaction. HSC70 plays an important role in chaperone-mediated autophagy (CMA), binding CMA substrates and transporting them to lysosomes. However, it has not been clarified whether HDAC10 is involved in CMA. In this study, we established the HDAC10 knockout HeLa cell line and evaluated its CMA activity to determine whether HDAC10 participates in regulating CMA. In HDAC10 knockout cells, lysosome-associated protein type 2A (LAMP2A) protein level increased and LAMP2A-positive lysosomes accumulated around the nucleus. Moreover, GAPDH, which is a well-known CMA substrate, was delivered to LAMP2A-positive lysosomes and degraded in HDAC10 knockout cells more efficiently than in wild type HeLa cells. These results suggest that CMA is activated in HDAC10 knockout cells. Meanwhile, turnover assay using LC3 and p62, which are macroautophagy markers, indicated that autophagic flux was fully functioning in HDAC10 knockout cells as well as in wild type HeLa cells. In conclusion, HDAC10 participated in regulating CMA, and HDAC10 knockout activated CMA and accelerated degradation of a CMA substrate.

1. Introduction

Autophagy is an evolutionarily conserved lysosomal degradation pathway by which cytoplasmic proteins and organelles are delivered to and degraded in the lysosome [1]. It is essential for cell survival, differentiation, development, and homeostasis [2,3]. Depending on the mode of cargo delivery to the lysosome, autophagy can be divided into three forms: macroautophagy, microautophagy, and chaperone-mediated autophagy (CMA) [1]. Macroautophagy is the most predominant type of autophagy and is characterized by the formation of autophagosome, which sequesters cytoplasmic content, including soluble materials and organelles. Later, the autophagosome fuses with the lysosome and becomes an autolysosome which degrades the materials contained within it [4]. In microautophagy, small components are transported into the lysosome by direct invagination of the lysosomal membrane and subsequent budding of vesicles into the lysosomal lumen [5]. During macroautophagy and microautophagy processes, cytosolic components are randomly engulfed in bulk. In contrast, CMA is a unique pathway by which cytosolic proteins are selectively transferred into the lysosome. Only CMA substrates which contain in their amino acid sequences a pentapeptide motif biochemically related to KFERQ, known as the CMA-targeting motif, can undergo degradation via CMA. The chaperone protein, heat shock cognate protein 70 kDa (HSC70), and co-chaperones specifically recognize the substrates containing the KFERQ motif and deliver them to the lysosome. At the lysosomal membrane, substrates bind to

lysosome-associated protein type 2A (LAMP2A) and this interaction drives the organization of LAMP2A into multimeric complexes required for substrate translocation into the lysosome [6]. However, CMA malfunctioning is linked to the pathogenesis of cancer and metabolic disorders and some neurodegenerative diseases, such as Parkinson's disease, Alzheimer disease, frontotemporal lobar degeneration, and Huntington disease [7]. CMA contributes to the degradation of neurodegeneration-related proteins which are prone to aggregate, and, consequently, a decline in CMA activity leads to the accumulation of toxic aggregates [7]. No effective treatment has been developed yet for these neurodegenerative diseases. Therefore, finding a way to activate CMA may help to prevent accumulation of neurodegeneration-related proteins, and would lead to the development of new treatments.

Histone deacetylases (HDACs) remove acetyl groups from lysine residues on histones, thus repressing gene transcription. Recent studies, however, have demonstrated that HDACs modify not only core histones but also nonhistone proteins. HDACs are divided into four classes, according to their homology to yeast HDACs: size, cellular localization, catalytic domain, and mechanism of action [8]. HDAC6 and HDAC10 are members of class IIb HDACs and similar in structure, but their subcellular localization and deacetylation targets are different. These facts suggest that HDAC10 and 6 likely have different functions [9].

Only few studies have investigated HDAC10 substrates and their functions. Previous reports indicated that HDAC10 plays a role in homologous recombination [10], suppresses cervical cancer metastasis [11], facilitates the cell cycle [12], and promotes autophagy [13]. Some studies have indicated that HDAC10 deacetylates HSC70 after interaction [8,13,14]. In experiments performed by Oehme et al., HDAC10 knockdown induced HSC70 acetylation and prevented autophagosome-lysosome fusion, which caused accumulation of autophagosomes [13]. As mentioned above, HSC70 is one of the major components of CMA. Nevertheless, whether HDAC10 is involved in regulation of CMA is unknown.

In this study, we established a HDAC10 knockout cell line and analyzed its CMA activity.

2. Materials and methods

2.1. Generation of HDAC10 knockout HeLa cell lines with CRISPR/Cas9 system

HeLa human cervical cancer cells were purchased from American Type Culture Collection and maintained in DMEM medium (Wako, Japan) containing 10% fetal bovine serum (FBS) and penicillin/streptomycin. We selected one predesigned CRISPR sequence against exon 1 of HDAC10 gene by using the Invitrogen GeneArt CRISPR Search and Design tool, and ordered oligonucleotide primers for guide RNA synthesis. The sequences of oligonucleotide primers were as follows:

(forward) F: 5′-TAATACGACTCACTATAGGACCGCGCTTGTGTAC-3′

(reverse) R: 5′-TTCTAGCTCTAAAACCATGGTACACAAGCGCGGT-3′

Guide RNA was produced using GeneArt Precision gRNA Synthesis Kit (Thermo Fisher, USA) according to manufacturer's protocol. Wild type (WT) HeLa cells were transfected with guide RNA and GeneArt Platinum Cas9 Nuclease (Thermo Fisher, USA) using Lipofectamine CRISPRMAX Cas9 Transfection Reagent (Thermo Fisher, USA). One week later, transfected cells were isolated by the limiting dilution method to obtain clones derived from a single-cell. Then, we analyzed the nucleotide sequences of the target DNA and HDAC10 protein levels.

2.2. Immunoblotting

Total cellular protein was extracted using NP-40 lysis buffer (50 mM Tris-HCl, pH 7.4, 150 mM NaCl, 1 mM EDTA, pH 8.0, 10% glycerol, and 1% NP-40) supplemented with complete mini protease inhibitors (Roche Diagnostic, Switzerland). Protein extracts were separated by 10% sodium dodecyl sulfate-polyacrylamide gel electrophoresis (SDS-PAGE). Then, the proteins were transferred onto methanol-activated polyvinylidene difluoride membranes (Wako Pure Chemical Industries, Japan) and probed with the following primary antibodies: anti-HDAC10 (Sigma-Aldrich, USA), anti-LAMP2A (Abcam, USA), anti-LC3 (MBL, Japan), anti-p62/SQSTM1 (MBL, Japan), and anti-actin beta antibodies (Bio-Rad, USA).

2.3. Quantitative Real-time PCR

RNA samples were purified using the Nucleospin RNA Kit (Takara Bio, Japan) and reverse transcribed into cDNA using Prime Script RT reagent Kit (Takara Bio, Japan). Quantitation of mRNA expression was performed according to the manufacturer's instructions using SYBR Green assay (Takara Bio, Japan) and the Bio-Rad CFX manager (Bio-Rad, USA). Forward and reverse primer sequences, respectively, were as follows:

LAMP2A; 5′-GCACAGTGAGCACAAATGAGT-3′, 5′-CAGTGGTGTG-TATGGTGGGT-3′

α-Actin; 5′-TAGACACCATGTGGGACGAAGACGAGA-3′ 5′-GCAGG-CACGTTGAAGGTCTAAACATGA-3′

2.4. Fluorescence microscopy

Cells on coverslips were fixed with 4% paraformaldehyde in PBS and were then permeabilized and blocked with 0.5% saponin, 5% normal goat serum, and 50 mM NH$_4$Cl in sodium glutamate buffer (20 mM PIPES-NaOH, 137 mM sodium glutamate, 2 mM MgCl$_2$; 1 mg/mL BSA, pH 6.8) for 4 h at 4 °C. Cells were incubated with anti-LAMP2A rabbit antibody, followed by Alexa 488-conjugated anti-rabbit IgG antibody. To label lysosomes, cells were incubated with culture medium containing 100 nM LysoTracker Red DND-99 (Invitrogen, USA) for 30 min at 37 °C before fixation. Fluorescence images were obtained using confocal microscope (FV1000D IX81, OLYMPUS, Japan).

2.5. Plasmids and cDNA transfection

We constructed plasmids containing the GAPDH-HaloTag (HT), as previously described [15]. Plasmid containing open reading frame of green fluorescent protein fused to that of LC3 (GFP-LC3) was kindly provided by Prof. Yao (Duke university, USA). Cells were transfected with X-tremeGENE HP DNA Transfection Reagent (Roche Diagnostic, Switzerland), according to the manufacturer's protocol.

2.6. Single-cell monitoring of CMA activity using the GAPDH-HT indicator

Cells grown on coverslips were transfected with GAPDH-HT plasmid. One day later, cells were incubated with culture medium containing 500 nM of tetramethylrhodamine (TMR) -HT ligand (Promega, USA) for 15 min at 37 °C, followed by three washes with PBS. Cells were fixed after labeling or after 24 h of cultivation.

Fluorescence images were obtained by using confocal microscope. Lysosomal translocation of GAPDH-HT was assessed by colocalization with LAMP2A protein staining. We quantitatively evaluated lysosomal accumulation of GAPDH-HT by counting the number of GAPDH-HT and LAMP2A dual positive puncta per cell [15].

2.7. Pulse chase assay

Cells were transfected with GAPDH-HT plasmid. Next day, transfected cells were pulse-labeled with 500 nM TMR-HT ligand for 15 min at 37 °C. To completely remove ligand from culture medium, cells were washed three times with PBS and culture medium was changed twice every 30 min, then chased for the indicated time. Harvested cells were lysed in NP-40 lysis buffer and centrifuged. An equal volume of supernatant per sample was separated with SDS-PAGE, then detection of GAPDH-HT by TMR-HT ligand was visualized with fluoro-image analyzer (Molecular Imager FX; Bio-Rad, USA).

2.8. Monitoring autophagic flux

For LC3 turnover assay, cells were cultured in DMEM with 10% FBS media in the presence or absence of bafilomycin A1 100 nM for 2 h. To confirm the starvation-induced reduction of p62 levels, cells were cultured in DMEM with 10% FBS media or in DMEM without amino acids for 2 h. Protein levels of LC3 and p62 were analyzed by immunoblotting.

2.9. Counting of GFP-LC3 puncta

Cells on coverslips were transfected with GFP-LC3 plasmid, and fixed with 4% paraformaldehyde in PBS 48 h after transfection. To induce macroautophagy, cells were treated with 100 nM rapamycin for 24 h before fixation. Fluorescence images were obtained using confocal microscope. The number of puncta per GFP-LC3-expressing cells was counted manually. Only cells displaying a modest over-expression level were included in the analysis.

2.10. Statistical analysis

Two-sample comparisons were conducted by Student's *t*-test. One-way ANOVA, followed by Tukey's HSD test, was used to determine multiple comparisons. Differences in the time dependent protein degradation between two groups were evaluated by two-way ANOVA with Tukey's HSD test. Statistical analyses were performed using a statistical software package (JMP Pro 13; SAS Institute, USA). $P < 0.05$ was considered statistically significant. All statistical results were presented as the mean ± standard error of the mean (SEM).

3. Results

3.1. LAMP2A expression increased in HDAC10 knockout cells

We used the CRISPR/Cas9 system and generated three HDAC10 knockout cell lines (#1−3). Immunoblotting with anti-HDAC10 antibody showed that the expression of HDAC10 protein was abolished in all HDAC10 knockout cell lines (Fig. 1A). However, we used HDAC10 knockout #1 in the following experiments, as both alleles of HDAC10 gene had single base deletion in exon 1.

First, we analyzed the level of LAMP2A expression, because its level in lysosomes correlated well with changes in CMA activity [16]. LAMP2A protein expression and mRNA expression were increased in HDAC10 knockout cells (Fig. 1A, B, and C). Second, we observed the subcellular location of LAMP2A-positive lysosomes by immunocytochemistry, since activation of CMA was associated with the mobilization of LAMP2A-enriched lysosomes to the perinuclear region of the cell [17]. Fluorescence images indicated that the number of lysosomes stained with both LysoTracker and anti-LAMP2A antibody increased in HDAC10 knockout cells.
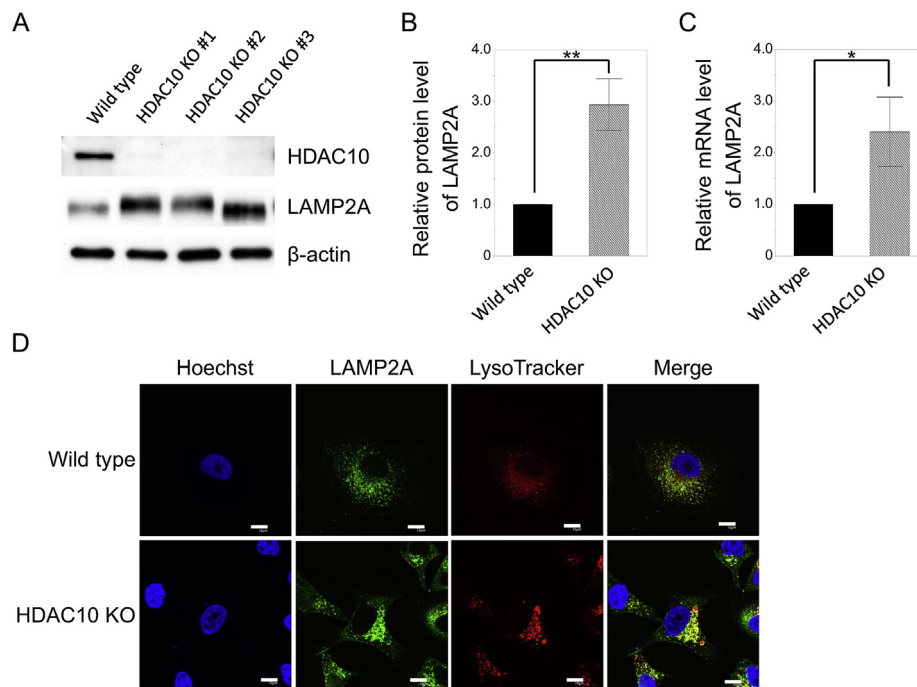

Fig. 1. The expression of LAMP2A increased in HDAC10 knockout cells. (A) HDAC10 and LAMP2A protein levels were assessed by immunoblotting. (B) LAMP2A protein expression levels were quantified by densitometric analysis. (C) The relative LAMP2A mRNA expression levels were assessed by Quantitative Real-time PCR. Data are the means ± SEM of three independent experiments; *$P < 0.05$ and **$P < 0.005$ (Student's *t*-test). (D) Representative immunofluorescence images of cells stained with antibody against LAMP2A (green), and with LysoTracker (red) and Hoechst 33342 (blue). Scale bar = 10 μm.
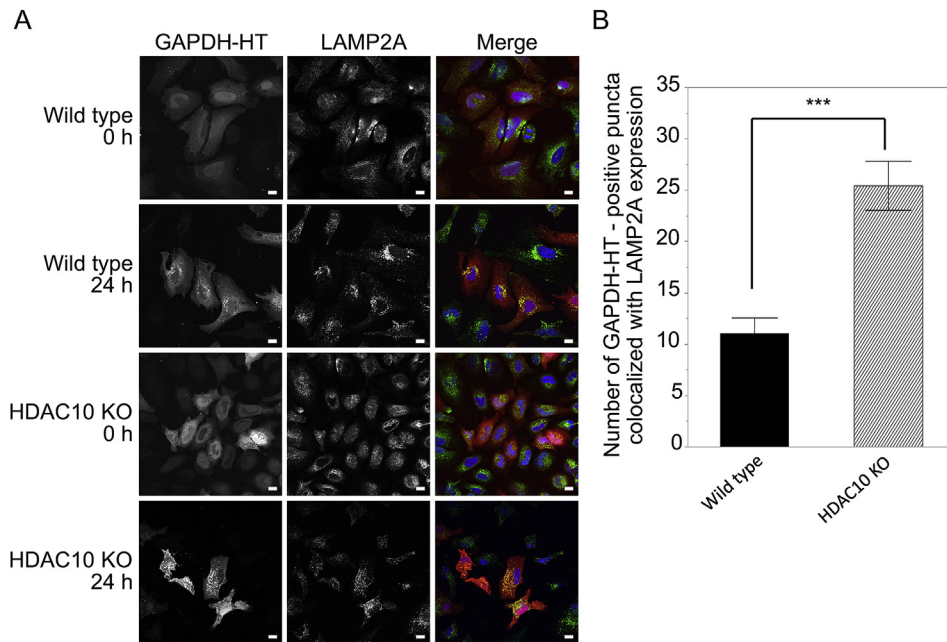
Fig. 2. HDAC10 knockout promoted the translocation of GAPDH to LAMP2A-positive lysosomes. (A) Representative fluorescence images of wild type HeLa cells and HDAC10 knockout cells at 0 h and 24 h after labeling GAPDH-HT with TMR-HT ligand (left) and LAMP2A by immunostaining (middle). Merge of the images (right): red for GAPDH-HT, green for LAMP2A, yellow for co-localization. Scale bar = 10 μm. (B) Quantitative analysis of GAPDH-HT lysosomal translocation. The number of GAPDH-HT and LAMP2A double-positive puncta per cell was calculated. Data are the means ± SEM of three independent experiments; ***$P < 0.0001$ (Student's t-test, n = 64 for wild type, and n = 67 for HDAC10 knockout).

Furthermore, LAMP2A-positive lysosomes accumulated around the nucleus more markedly in HDAC10 knockout cells than in WT HeLa cells (Fig. 1D). These data suggested that CMA activity was upregulated in HDAC10 knockout cells compared to WT cells.

3.2. HDAC10 knockout promoted the translocation of GAPDH to LAMP2A-positive lysosomes

Changes in the abundance of key CMA components and in the amount and distribution of CMA-related lysosomes can indirectly assess CMA activity. However, to directly investigate the CMA activity at a single-cell level, we utilized the GAPDH-HaloTag (HT) indicator system, which could monitor the translocation of GAPDH, a well-known CMA substrate, from cytoplasm to lysosomes [15,18]. TMR-labeled GAPDH-HT was uniformly distributed in the cytoplasm at the time of labeling, but 24 h after initial incubation led to puncta-like accumulations of GAPDH-HT in both cell lines, WT and HDAC10 knockout. Almost all labeled GAPDH-HT puncta were colocalized with LAMP2A at 24 h, as confirmed by double immunostaining (Fig. 2A). Comparison of the number of GAPDH-HT puncta colocalized with LAMP2A between WT and HDAC10 knockout cells resulted in a significantly higher number of GAPDH-HT puncta per cell in HDAC10 knockout cells (Fig. 2B). These results indicated that the translocation of GAPDH to CMA-related lysosomes was activated in HDAC10 knockout cells.

3.3. HDAC10 knockout accelerated GAPDH degradation rate

Moreover, we performed pulse chase assay using GAPDH-HT and TMR-HT ligands to assess whether HDAC10 knockout also promoted the decomposition of GAPDH. The amount of TMR-HT ligand that labeled GAPDH-HT remained unchanged in WT cells, whereas it significantly decreased in HDAC10 knockout cells (Fig. 3A and B). This result suggested that HDAC10 knockout accelerated the degradation rate of GAPDH.

3.4. HDAC10 knockout did not affect macroautophagy

The term "autophagic flux" is used to denote overall autophagic degradation rather than autophagosome formation. LC3 is
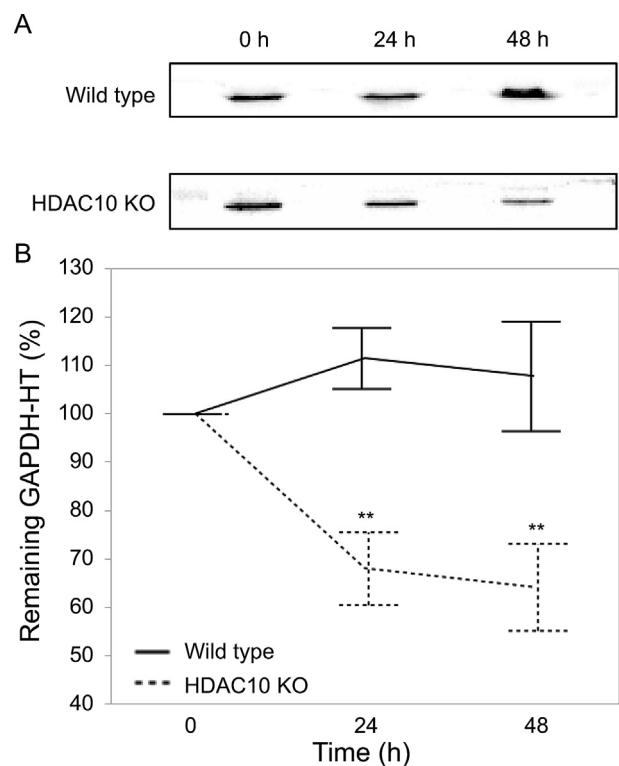

Fig. 3. HDAC10 knockout accelerated the degradation rate of GAPDH. (A) Representative images of GAPDH-Halo tag pulse chase assay. (B) Quantified data for Halo tag pulse chase assay. Data are the means ± SEM of five independent experiments; **$P < 0.005$ (Two-way ANOVA with Tukey's HSD test).
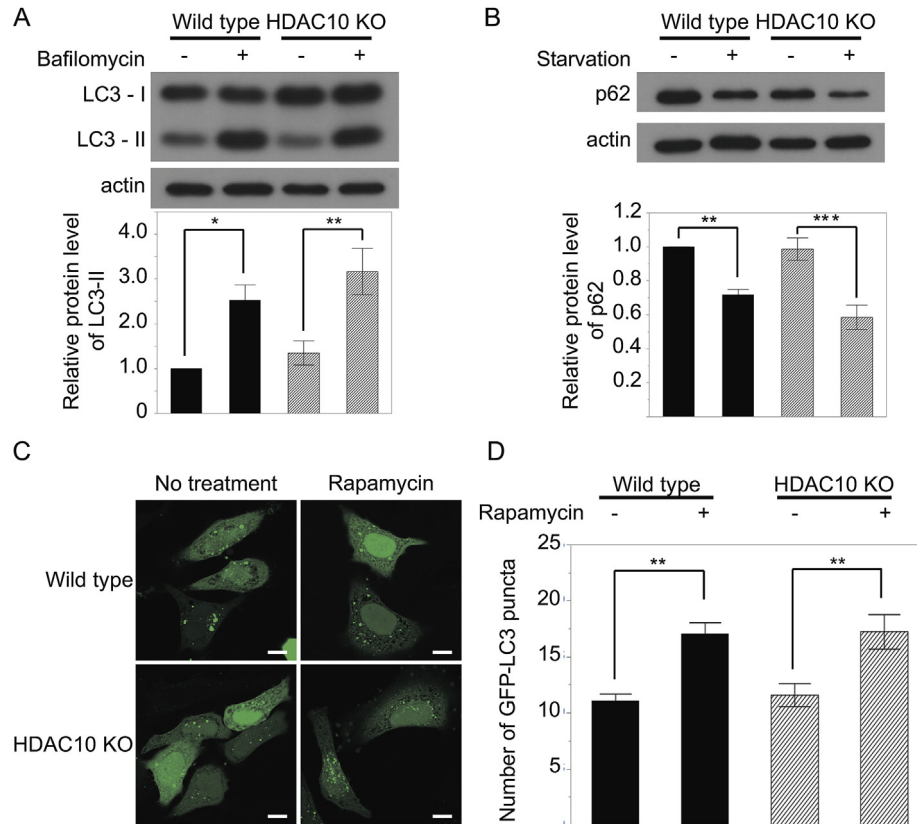
Fig. 4. HDAC10 knockout did not affect macroautophagy. (A) LC3-II and (B) p62 protein levels were assessed by immunoblotting. Protein expression levels were quantified by densitometric analysis. Data are expressed by the means ± SEM of nine independent experiments; *$P < 0.05$, **$P < 0.005$, ***$P < 0.0001$ (Tukey's HSD test). (C) Representative images of GFP-LC3-expressing cells cultured in the presence or absence of rapamycin. Scale bar = 10 μm. (D) Quantification of the number of GFP-LC3 puncta per cell. Data are expressed by the means ± SEM of three independent experiments; **$P < 0.005$ (Tukey's HSD test, n = 34 for HDAC10 knockout in the presence of rapamycin, and n = 38 for others).

currently the most widely used autophagosome marker because the amount of LC3-II reflects the number of autophagosomes and autophagy-related structures. However, the number of autophagic organelles at a given moment is regulated by autophagosome formation and degradation upon fusion with lysosomes. Thus, the amount of LC3-II at a certain time point does not necessarily indicate the degree of autophagic flux [19]. Therefore, to compare the autophagic activity in HDAC10 knockout cells with that in WT cells, we performed the LC3 turnover assay as it measures autophagic flux. Immunoblotting showed that the LC3-II level in HDAC10 knockout cells was slightly higher or equal to that in WT cells, but bafilomycin treatment led to a significant and equivalent increase of LC3-II levels in both cell lines (Fig. 4A). These data suggested that autophagic flux functioned normally in HDAC10 knockout and WT cells. We also checked p62 levels because it is another widely used marker to monitor autophagic activity. The amount of p62 was significantly and similarly decreased by starvation in both cell lines under the same conditions (Fig. 4B). These results indicated that HDAC10 knockout cells were not impaired in autophagic flux.

Then we counted the number of GFP-LC3 puncta per cell which accurately measures autophagosome numbers. Under normal growth conditions, the number of GFP-LC3 puncta in HDAC10 knockout cells was almost the same as that in WT cells (Fig. 4C and D). Administration of rapamycin, which is mTOR inhibitor and induces autophagy, significantly increased the number of GFP-LC3 puncta in both cell lines. However, no significant difference in the number of GFP-LC3 puncta between both cell lines was observed under neither condition, which agreed with the result of LC3-II and p62 immunoblotting. These results indicated that HDAC10

knockout did not affect autophagosome formation.

4. Discussion

The purpose of the present study was to investigate whether HDAC10 affected CMA activity. Indeed, we have demonstrated that HDAC10 knockout activated CMA and accelerated the degradation rate of a CMA substrate. This is the first report which showed that HDAC10 participated in regulating CMA activity. Thus, inhibition of HDAC10 expression may be effective to treat neurodegenerative diseases of which CMA downregulation is the main associated cause.

The downstream targets of HDAC10 are incompletely characterized, therefore it is unknown how HDAC10 regulates CMA activity. Two hypothetical mechanisms of CMA regulation by HDAC10 were proposed. First, HSC70 acetylation, induced by HDAC10 knockout, may promote CMA activation, because HSC70 was proposed as a target of HDAC10 [8,13,14]. HSC70 is present in cytosol and lysosomes and plays important roles in each subcellular location [20]. Cytosolic HSC70 recognizes CMA substrates and delivers them to the lysosomal surface. Meanwhile, lysosomal HSC70, which is located at the cytosolic side of the lysosomal membrane and in the lysosomal lumen, is required for substrate unfolding and translocation into the lysosome [21−23]. Lysosomes containing HSC70 are active for CMA, whereas lysosomes lacking HSC70 are unable to perform CMA [24]. Taken together, HSC70 is essential to activate CMA. Further research is needed to elucidate how deacetylation of HSC70 by HDAC10 could function in CMA, and which steps in CMA are facilitated by HSC70 acetylation. Second, HDAC10

may be involved in AKT pathway which regulates CMA. Dynamics of LAMP2A assembly and disassembly depend on glial fibrillary acidic protein (GFAP) phosphorylation status. Unmodified GFAP binds to LAMP2A at the multimeric complex and contributes to its stabilization [25]. During stress conditions, the "pleckstrin homology domain leucine-rich repeat protein phosphatase 1" (PHLPP1) protein is recruited to the lysosomal membrane, dephosphorylating AKT, and then activating CMA, which is then followed by GFAP dephosphorylation through AKT dephosphorylation [26]. Interestingly, Yang et al. reported that HDAC10 interacted with AKT, and HDAC10 knockdown significantly decreased the phosphorylation of AKT in a lung cancer cell line [27]. Furthermore, another report indicated that tubastatin, which is a HDAC6 and 10 inhibitor, repressed AKT phosphorylation by increasing AKT-PHLPP1 association [28]. These reports supported our hypothesis that inhibition of HDAC10 upregulated CMA via PHLPP1-AKT-GFAP pathway.

Our data indicated no significant difference in macroautophagy activity between WT and HDAC10 knockout cells, which disagreed with results reported by Oehme et al. They concluded that HDAC10 contributed to autophagosome-lysosome fusion in a neuroblastoma cell line, because HDAC10 depletion by transient siRNA transfection disabled the fusion of autophagosomes to lysosomes and thus caused accumulation of autophagosomes [13]. If the fusion of autophagosomes to lysosomes was impaired in HDAC10 knockout cells, LC3-II levels would have not changed with bafilomycin treatment, and the number of GFP-LC3 puncta in HDAC10 knockout cells would have increased by rapamycin treatment more than that in WT cells. However, the LC3-II level was increased by bafilomycin in HDAC10 knockout, and the number of GFP-LC3 puncta in HDAC10 knockout and WT cell were similar regardless of rapamycin treatment. Concerning the difference, we speculated that the failure of autophagosome-lysosome fusion could be compensated by other molecules in our long-term HDAC10 knockout cell, in contrast to their transient HDAC10 knockdown cell.

A limitation of our study is that the examinations using the GAPDH-HT indicator detected both CMA and a certain microautophagy activity. Recently, endosomal microautophagy involving HSC70 has been described [29]. In this process, cytosolic soluble proteins are incorporated into late endosomes/multivesicular bodies in an HSC70 dependent manner. GAPDH is recognized by HSC70 and incorporated into late endosomes by microautophagy [29]. To selectively evaluate CMA activity, we examined the number of GAPDH-HT puncta colocalizing with LAMP2A in the fluorescence microscopy experiment. However, in the pulse chase assay, we were unable to separately measure CMA and microautophagy. A recent study has reported that CMA and microautophagy activities can be separately assessed by knockdown of microautophagy- and CMA-related proteins, respectively [30]. Thus, we could perform that methodology to confirm our results.

In conclusion, we showed that HDAC10 knockout activated CMA and accelerated the protein degradation through CMA pathway. Inhibition of HDAC10 function may be useful for treatment of neurodegenerative diseases which result from CMA impairment. Further research on elucidating the molecular mechanism by which HDAC10 regulates CMA activity is needed.

Funding

Author contributions

All authors contributed to drafting and/or revising the article, and approved the final version intended for publication.

Acknowledgments

Transparency document

Transparency document related to this article can be found online at https://doi.org/10.1016/j.bbrc.2019.12.048.

References

[1] B. Levine, G. Kroemer, Autophagy in the pathogenesis of disease, Cell 132 (2008) 27–42, https://doi.org/10.1016/j.cell.2007.12.018.

[2] N. Mizushima, B. Levine, A.M. Cuervo, D.J. Klionsky, Autophagy fights disease through cellular self-digestion, Nature 451 (2008) 1069–1075, https://doi.org/10.1038/nature06639.

[3] N. Mizushima, B. Levine, Autophagy in mammalian development and differentiation, Nat. Cell Biol. 12 (2010) 823–830, https://doi.org/10.1038/ncb0910-823.

[4] N. Mizushima, M. Komatsu, Autophagy: renovation of cells and tissues, Cell 147 (2011) 728–741, https://doi.org/10.1016/j.cell.2011.10.026.

[5] J.B. Kunz, H. Schwarz, A. Mayer, Determination of four sequential stages during microautophagy in vitro, J. Biol. Chem. 279 (2004) 9987–9996, https://doi.org/10.1074/jbc.M307905200.

[6] S.J. Orenstein, A.M. Cuervo, Chaperone-mediated autophagy: molecular mechanisms and physiological relevance, Semin. Cell Dev. Biol. 21 (2010) 719–726, https://doi.org/10.1016/j.semcdb.2010.02.005.

[7] S. Kaushik, A.M. Cuervo, The coming of age of chaperone-mediated autophagy, Nat. Rev. Mol. Cell Biol. 19 (2018) 365–381, https://doi.org/10.1038/s41580-018-0001-6.

[8] G. Pinto, B. Shtaif, M. Phillip, G. Gat-Yablonski, Growth attenuation is associated with histone deacetylase 10-induced autophagy in the liver, J. Nutr. Biochem. 27 (2016) 171–180, https://doi.org/10.1016/j.jnutbio.2015.08.031.

[9] A.R. Guardiola, T.P. Yao, Molecular cloning and characterization of a novel histone deacetylase HDAC10, J. Biol. Chem. 277 (2002) 3350–3356, https://doi.org/10.1074/jbc.M109861200.

[10] S. Kotian, S. Liyanarachchi, A. Zelent, J.D. Parvin, Histone deacetylases 9 and 10 are required for homologous recombination, J. Biol. Chem. 286 (2011) 7722–7726, https://doi.org/10.1074/jbc.C110.194233.

[11] C. Song, S. Zhu, C. Wu, J. Kang, Histone deacetylase (HDAC) 10 suppresses cervical cancer metastasis through inhibition of matrix metalloproteinase (MMP) 2 and 9 expression, J. Biol. Chem. 288 (2013) 28021–28033, https://doi.org/10.1074/jbc.M113.498758.

[12] Y. Li, L. Peng, E. Seto, Histone deacetylase 10 regulates the cell cycle G2/M phase transition via a novel Let-7-HMGA2-Cyclin A2 pathway, Mol. Cell. Biol. 35 (2015) 3547–3565, https://doi.org/10.1128/mcb.00400-15.

[13] I. Oehme, J.P. Linke, B.C. Bock, T. Milde, M. Lodrini, B. Hartenstein, I. Wiegand, C. Eckert, W. Roth, M. Kool, S. Kaden, H.J. Grone, J.H. Schulte, S. Lindner, A. Hamacher-Brady, N.R. Brady, H.E. Deubzer, O. Witt, Histone deacetylase 10 promotes autophagy-mediated cell survival, Proc. Natl. Acad. Sci. U.S.A. 110 (2013) E2592–E2601, https://doi.org/10.1073/pnas.1300113110.

[14] I.L. Lai, T.P. Lin, Y.L. Yao, C.Y. Lin, M.J. Hsieh, W.M. Yang, Histone deacetylase 10 relieves repression on the melanogenic program by maintaining the deacetylation status of repressors, J. Biol. Chem. 285 (2010) 7187–7196, https://doi.org/10.1074/jbc.M109.061861.

[15] T. Seki, K.I. Yoshino, S. Tanaka, E. Dohi, T. Onji, K. Yamamoto, I. Hide, H.L. Paulson, N. Saito, N. Sakai, Establishment of a novel fluorescence-based method to evaluate chaperone-mediated autophagy in a single neuron, PLoS One 7 (2012), e31232, https://doi.org/10.1371/journal.pone.0031232.

[16] E. Arias, Methods to study chaperone-mediated autophagy, Methods Enzymol. 588 (2017) 283–305, https://doi.org/10.1016/bs.mie.2016.10.009.

[17] S. Kaushik, A.M. Cuervo, Methods to monitor chaperone-mediated autophagy, Methods Enzymol. 452 (2009) 297–324, https://doi.org/10.1016/s0076-6879(08)03619-7.

[18] E. Dohi, S. Tanaka, T. Seki, T. Miyagi, I. Hide, T. Takahashi, M. Matsumoto, N. Sakai, Hypoxic stress activates chaperone-mediated autophagy and modulates neuronal cell survival, Neurochem. Int. 60 (2012) 431–442, https://doi.org/10.1016/j.neuint.2012.01.020.

[19] P. Jiang, N. Mizushima, LC3- and p62-based biochemical methods for the analysis of autophagy progression in mammalian cells, Methods 75 (2015) 13–18, https://doi.org/10.1016/j.ymeth.2014.11.021.

[20] F. Stricher, C. Macri, M. Ruff, S. Muller, HSPA8/HSC70 chaperone protein: structure, function, and chemical targeting, Autophagy 9 (2013) 1937–1954, https://doi.org/10.4161/auto.26448.

[21] F.A. Agarraberes, S.R. Terlecky, J.F. Dice, An intralysosomal hsp 70 is required for a selective pathway of lysosomal protein degradation, J. Cell Biol. 137 (1997) 825–834, https://doi.org/10.1083/jcb.137.4.825.

[22] N. Salvador, C. Aguado, M. Horst, E. Knecht, Import of a cytosolic protein into lysosomes by chaperone-mediated autophagy depends on its folding state, J. Biol. Chem. 275 (2000) 27447−27456, https://doi.org/10.1074/jbc.M001394200.

[23] F.A. Agarraberes, J.F. Dice, A molecular chaperone complex at the lysosomal membrane is required for protein translocation, J. Cell Sci. 114 (2001) 2491−2499.

[24] A.M. Cuervo, J.F. Dice, E. Knecht, A population of rat liver lysosomes responsible for the selective uptake and degradation of cytosolic proteins, J. Biol. Chem. 272 (1997) 5606−5615, https://doi.org/10.1074/jbc.272.9.5606.

[25] U. Bandyopadhyay, S. Sridhar, S. Kaushik, R. Kiffin, A.M. Cuervo, Identification of regulators of chaperone-mediated autophagy, Mol. Cell 39 (2010) 535−547, https://doi.org/10.1016/j.molcel.2010.08.004.

[26] E. Arias, H. Koga, A. Diaz, E. Mocholi, B. Patel, A.M. Cuervo, Lysosomal mTORC2/PHLPP1/Akt regulate chaperone-mediated autophagy, Mol. Cell 59 (2015) 270−284, https://doi.org/10.1016/j.molcel.2015.05.030.

[27] Y. Yang, Y. Huang, Z. Wang, H.T. Wang, B. Duan, D. Ye, C. Wang, R. Jing, Y. Leng, J. Xi, W. Chen, G. Wang, W. Jia, S. Zhu, J. Kang, HDAC10 promotes lung cancer proliferation via AKT phosphorylation, Oncotarget 7 (2016) 59388−59401, https://doi.org/10.18632/oncotarget.10673.

[28] S. Saito, Y. Zhuang, B. Shan, S. Danchuk, F. Luo, M. Korfei, A. Guenther, J.A. Lasky, Tubastatin ameliorates pulmonary fibrosis by targeting the TGFbeta-PI3K-Akt pathway, PLoS One 12 (2017), e0186615, https://doi.org/10.1371/journal.pone.0186615.

[29] R. Sahu, S. Kaushik, C.C. Clement, E.S. Cannizzo, B. Scharf, A. Follenzi, I. Potolicchio, E. Nieves, A.M. Cuervo, L. Santambrogio, Microautophagy of cytosolic proteins by late endosomes, Dev. Cell 20 (2011) 131−139, https://doi.org/10.1016/j.devcel.2010.12.003.

[30] M. Sato, T. Seki, A. Konno, H. Hirai, Y. Kurauchi, A. Hisatsune, H. Katsuki, Fluorescent-based evaluation of chaperone-mediated autophagy and micro-autophagy activities in cultured cells, Genes Cells 21 (2016) 861−873, https://doi.org/10.1111/gtc.12390.